



Contents lists available at ScienceDirect

Infrared Physics & Technology

journal homepage: www.elsevier.com/locate/infrared

Regular article

Resonant detectors and focal plane arrays for infrared detection

K.K. Choi^{a,*}, S.C. Allen^b, J.G. Sun^a, E.A. DeCuir^a^aU.S. Army Research Laboratory, Adelphi, MD 20783, United States^bL-3 Communications - Cincinnati Electronics, Mason, OH 45040, United States

HIGHLIGHTS

- Demonstrated resonator-QWIPs for narrowband and broadband long wavelength infrared detection.
- Using a low doping and a thin active layer thickness, quantum efficiency between 25 and 37% is achieved.
- BLIP temperature is 65 K with a cutoff wavelength up to 11 μm .
- High quality, 1-megapixel infrared images were obtained.

ARTICLE INFO

Article history:

Received 27 September 2016

Revised 6 December 2016

Accepted 7 December 2016

Available online xxxxx

Keywords:

QWIP

Resonance

FPA

Electromagnetic modeling

Quantum efficiency

ABSTRACT

We are developing resonator-QWIPs for narrowband and broadband long wavelength infrared detection. Detector pixels with 25 μm and 30 μm pitches were hybridized to fanout circuits and readout integrated electronics for radiometric measurements. With a low to moderate doping of $0.2\text{--}0.5 \times 10^{18} \text{ cm}^{-3}$ and a thin active layer thickness of 0.6–1.3 μm , we achieved a quantum efficiency between 25 and 37% and a conversion efficiency between of 15 and 20%. The temperature at which photocurrent equals dark current is about 65 K under F/2 optics for a cutoff wavelength up to 11 μm . The NE Δ T of the FPAs is estimated to be 20 mK at 2 ms integration time and 60 K operating temperature. This good performance confirms the advantages of the resonator-QWIP approach.

© 2016 Published by Elsevier B.V.

1. Introduction

We have established a highly reliable and accurate electromagnetic (EM) model to calculate the quantum efficiency (QE) of an infrared detector [1]. In this work, we apply it to design narrowband as well as broadband resonator-quantum well infrared photodetectors (R-QWIPs) [2]. The R-QWIP structure uses the active pixel volume as a resonator to store the incident light until the light is absorbed. By cycling light in the detector volume, a large QE can be obtained even with a thin and weakly absorbing material. With this special detector characteristic, the present detectors are designed to have small active layer thickness t_{ac} ranging from 0.6 μm to 1.3 μm and low doping density N_D in the well ranging from 0.2 to 0.5 (in the unit of 10^{18} cm^{-3} used throughout this paper). Despite these small t_{ac} and N_D , the observed QE is in the range of 25–37%. This result thus exemplifies the advantages of R-QWIPs.

2. Narrowband R-QWIPs

For the narrowband design, we use a standard QWIP material, which consists of 15 periods of 56 Å GaAs/600 Å $\text{Al}_{0.2}\text{Ga}_{0.8}\text{As}$ sandwiched between a top and a bottom GaAs contact layers. The active layer thickness t_{ac} is thus about 1.0 μm . There are also thin layers of $\text{Al}_{0.4}\text{Ga}_{0.6}\text{As}$ in the material stack for the etch-stop purposes. The material is designed to detect at a peak wavelength λ_{peak} of 10.6 μm with a 1 μm bandwidth. The absorption coefficient α of the materials with different N_D is calculated from the standard transfer matrix method [3,4] and is shown in Fig. 1. The peak α varies from 0.05 μm^{-1} to 0.2 μm^{-1} when N_D increases from 0.2 to 0.8. Since these materials have a long cutoff λ_c at 11.2 μm , the dark current is expected to be high. We therefore choose small N_D of 0.2 (labeled as Det. A) and 0.3 (labeled as Det. B) to lower the dark current. At the same time, the adopted thin layer will yield a large photoconductive gain, which is known to be inversely proportional to the number of QWs. With a large photocurrent provided by large resonant QE and gain and a low dark current provided by low doping, the operating temperature of a QWIP can be increased.

* Corresponding author.

E-mail address: kwong.k.choi.civ@mail.mil (K.K. Choi).

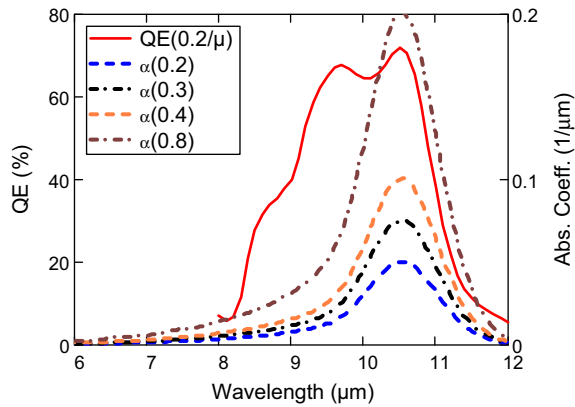


Fig. 1. The theoretical QE (solid curve) of an R-QWIP with $t_{ac} = 1.4 \mu\text{m}$ and a constant α of $0.2 \mu\text{m}^{-1}$. The dashed curves shows the theoretical α for different N_D (in the unit of 10^{18}cm^{-3}).

The designed material structures were grown by IntelliEPI, Inc. The material detection spectra were characterized at the company using $1 \text{mm} \times 1 \text{mm}$ large area devices (LADs). Each LAD is covered with a metallic grid of variable spacing ranging from $60 \mu\text{m}$ to $100 \mu\text{m}$. This grid scatters the top illuminated light into the detector. Due to the presence of multiple grid spacing, this light coupling scheme does not depend on the incident wavelength, and its spectral lineshape reflects the material intrinsic absorption spectrum. Fig. 2 shows the measured LAD spectra for Det. A and Det. B at 0.6V substrate voltage and 77K operating temperature. They match closely with the designed α lineshape.

With the known spectral response, we then design a matching resonant geometry using electromagnetic modeling. Our modeling uses finite element method (FEM) to solve Maxwell's equation,

$$\nabla \times (\mu_r^{-1} \nabla \times \mathbf{E}) - k_0^2 \epsilon_{rc} \mathbf{E} = 0, \quad (1)$$

via trial basis functions under a user defined boundary condition. In Eq. (1), μ_r and $\epsilon_{rc} = \epsilon_r - j\epsilon_i$ are the relative permeability and relative

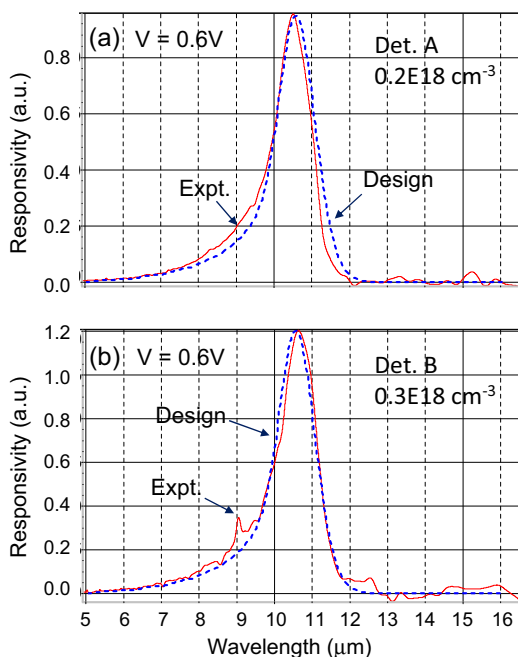


Fig. 2. The measured LAD lineshape (solid curve) of (a) Det. A and (b) Det. B. Both are very close to the designed α lineshape (dashed curve).

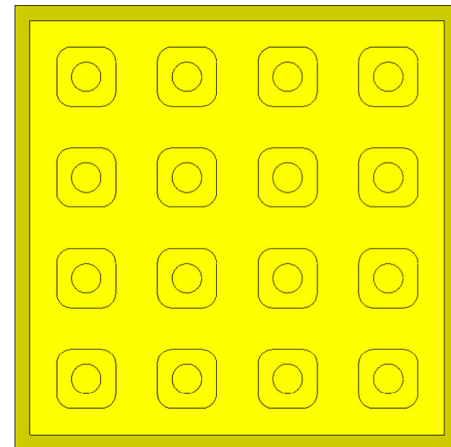
permittivity, respectively, and $k_0 = 2\pi/\lambda$ is the free space wavevector. Through variational principles, FEM transforms Eq. (1) into a large set of linear equations, with which Eq. (1) can be solved by matrix multiplication. To yield a valid solution, it is important to adopt correct boundary conditions in the model.

The present modeling is performed in the RF Module of a commercial EM solver, COMSOL Multiphysics. The modeling procedures involve selecting the EM analysis mode, building the 3D detector geometry, defining constants, variables, and functions, inputting subdomain properties, selecting appropriate boundary conditions, building mesh structures, setting solver parameters, performing computation, and using post processing to yield the required information. The calculated quantity is the detector absorption quantum efficiency η via

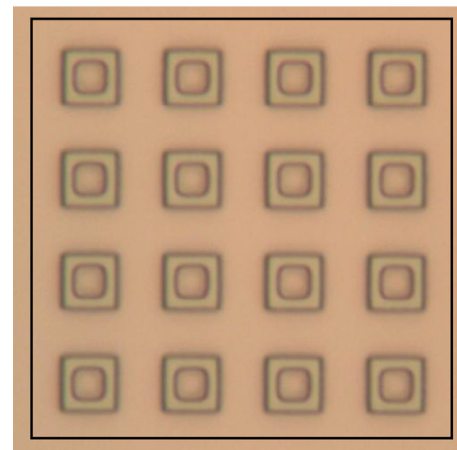
$$\eta(\lambda) = \frac{n(\lambda)\alpha(\lambda)}{AE_0^2} \int_V |E_z(\mathbf{r})|^2 d^3r, \quad (2)$$

where $n(\lambda)$ is the material refractive index, $\alpha(\lambda)$ is the material absorption coefficient, V is the detector active volume, A is the detector area, E_0 is the incident optical electric field, and $E_z(\mathbf{r})$ is the vertical optical electric field inside the active volume.

The designed resonant structure for light coupling is shown in Fig. 3a. In this design, the pixel pitch is $30 \mu\text{m}$ and the linear pixel size is $28 \mu\text{m}$. A set of rings are fabricated into the top contact layer and they are covered with gold. The detector substrate is



(a) Designed



(b) Realized

Fig. 3. The designed and the fabricated R-QWIP pixel.

Download English Version:

<https://daneshyari.com/en/article/5488540>

Download Persian Version:

<https://daneshyari.com/article/5488540>

[Daneshyari.com](https://daneshyari.com)